

DTIC COPY

(4)

AD-A204 235 —

# David Taylor Research Center

Bethesda, MD 20084-5000

DTRC-88/042 December 1988

Computation, Mathematics and Logistics Department  
Research and Development Report

## The "Bubble" Concept of Axisymmetric Vortex Breakdown With and Without Obstacles in the Vortex Core

by

Hans J. Lugt

Joseph J. Gorski

DTRC-88/042 The "Bubble" Concept of Axisymmetric Vortex Breakdown With and  
Without Obstacles in the Vortex Core



DTIC  
SELECTED  
FEB 06 1989  
S H D

Approved for public release; distribution is unlimited.

89 2 6 003

UNCLASSIFIED

SECURITY CLASSIFICATION OF THIS PAGE

AD A 204 235

## REPORT DOCUMENTATION PAGE

1a. REPORT SECURITY CLASSIFICATION UNCLASSIFIED		1b. RESTRICTIVE MARKINGS	
2a. SECURITY CLASSIFICATION AUTHORITY		3. DISTRIBUTION/AVAILABILITY OF REPORT Approved for public release; distribution is unlimited.	
2b. DECLASSIFICATION/DOWNGRADING SCHEDULE			
4. PERFORMING ORGANIZATION REPORT NUMBER(S) DTRC-88/042		5. MONITORING ORGANIZATION REPORT NUMBER(S)	
6a. NAME OF PERFORMING ORGANIZATION David Taylor Research Center	6b. OFFICE SYMBOL (If applicable) Code 1802	7a. NAME OF MONITORING ORGANIZATION	
6c. ADDRESS (City, State, and ZIP Code) Bethesda, Maryland 20084-5000		7b. ADDRESS (City, State, and ZIP Code)	
8a. NAME OF FUNDING/SPONSORING ORGANIZATION Office of Naval Research	8b. OFFICE SYMBOL (If applicable)	9. PROCUREMENT INSTRUMENT IDENTIFICATION NUMBER	
8c. ADDRESS (City, State, and ZIP Code) Arlington, Virginia 22217		10. SOURCE OF FUNDING NUMBERS	
		PROGRAM ELEMENT NO. 61152N	PROJECT NO. Z PRO0000101
		TASK NO.	WORK UNIT ACCESSION NO. DN507044
11. TITLE (Include Security Classification) The "Bubble" Concept of Axisymmetric Vortex Breakdown With and Without Obstacles in the Vortex Core			
12. PERSONAL AUTHOR(S) Lugt, Hans J. and Gorski, Joseph, J.			
13a. TYPE OF REPORT Final	13b. TIME COVERED FROM _____ TO _____	14. DATE OF REPORT (Year, Month, Day) 1988 December	15. PAGE COUNT 35
16. SUPPLEMENTARY NOTATION Use semi-colons separators			
17. COSATI CODES		18. SUBJECT TERMS (Continue on reverse if necessary and identify by block number) Vortex Control, Vortex Breakdown	
FIELD	GROUP	SUB-GROUP	
19. ABSTRACT (Continue on reverse if necessary and identify by block number) There is now sufficient evidence that axisymmetric recirculation zones in the form of "bubbles" on the axis of rotation of a vortex can be steady-state and stable. It appears also that the majority of researchers accept these bubbles as a form or a part of vortex breakdown. However, a gray area with regard to the definition of vortex breakdown exists when no stagnation point at the axis of rotation occurs. To use the appearance of such a stagnation point as a criterion for vortex breakdown might be too restrictive. The situation becomes even more aggravated when an obstacle is placed on the axis of rotation. Are re-circulation (or separation) regions in the front and rear of the obstacle indications of vortex breakdown or of Taylor-Proudman columns? This report addresses some of the problems in context with vortex control. (Key word: Vortex control. (code) A)			
20. DISTRIBUTION/AVAILABILITY OF ABSTRACT <input type="checkbox"/> UNCLASSIFIED/UNLIMITED <input checked="" type="checkbox"/> SAME AS RPT <input type="checkbox"/> DTIC USERS		21. ABSTRACT SECURITY CLASSIFICATION UNCLASSIFIED	
22a. NAME OF RESPONSIBLE INDIVIDUAL Hans J. Lugt		22b. TELEPHONE (Include Area Code) (202) 227-1925	22c. OFFICE SYMBOL Code 1802

## CONTENTS

	<i>Page</i>
<b>ABSTRACT</b> .....	1
<b>ADMINISTRATIVE INFORMATION</b> .....	1
<b>INTRODUCTION</b> .....	1
<b>DESCRIPTION OF THE FLOW MODEL AND NUMERICAL ALGORITHM</b> .....	4
<b>RESULTS</b> .....	6
<b>CONCLUSIONS</b> .....	8
<b>REFERENCES</b> .....	27

## FIGURES

1. Sketches of steady-state meridional streamlines of axisymmetric vortex-breakdown bubbles .....	9
2. Spiral vortex breakdown in a turbulent swirling pipe flow behind an orifice made visible by a hollow-core cavitation of gas along the axis .....	10
3. Grid of the computational half-plane .....	11
4. Grid of the computational half-plane with a rod .....	11
5. Grid of the computational half-plane with a ring-shaped body at the axis "nozzle" .....	12
6. Grid of the computational half-plane with a sphere at the axis .....	12
7. Flow field for $Re = 500, S = 0.80$ .....	13
8. Flow field for $Re = 500, S = 0.82$ .....	14
9. Flow field for $Re = 500, S = 0.83$ .....	15
10. Flow field for $Re = 500, S = 0.85$ .....	16
11. Flow field for $Re = 500, S = 0.87$ .....	17
12. Flow field for $Re = 500, S = 1.05$ .....	18
13. $w$ -component at the axis of rotation for $Re = 500, S = 1.05$ .....	19
14. Flow field for $Re = 2500, S = 0.85$ .....	20

By	
Distribution/	
Availability Codes	
Dist	Avail and/or Special
A-1	

## CONTENTS (Continued)

	Page
15. Meridional streamlines for $Re = 500, S = 0.80$ with a rod, $R_{st} = 0.1$ .....	21
16. Meridional streamlines for $Re = 500, S = 0.80$ with a rod, $R_{st} = 0.2$ .....	21
17. Meridional streamlines for $Re = 500, S = 0.82$ with a rod, $R_{st} = 0.1$ .....	22
18. Flow field for $Re = 500, S = 0.80$ with a nozzle .....	23
19. Flow field for $Re = 500, S = 0.82$ with a nozzle .....	24
20. Meridional streamlines for $Re = 500, S = 0.80$ with a sphere .....	25

## ABSTRACT

There is now sufficient evidence that axisymmetric recirculation zones in the form of "bubbles" on the axis of rotation of a vortex can be steady-state and stable. It appears also that the majority of researchers accept these bubbles as a form or a part of vortex breakdown. However, a gray area with regard to the definition of vortex breakdown exists when no stagnation point at the axis of rotation occurs. To use the appearance of such a stagnation point as a criterion for vortex breakdown might be too restrictive. The situation becomes even more aggravated when an obstacle is placed on the axis of rotation. Are recirculation (or separation) regions in the front and rear of the obstacle indications of vortex breakdown or of Taylor-Proudman columns? This report addresses some of the problems in context with vortex control.

## ADMINISTRATIVE INFORMATION

This project was supported by the DTRC Independent Research Program, sponsored by the Office of the Chief of Naval Research, and administered by the Research Director, DTRC 0113, under Program Element 61152N, Task Area ZR-000-01-01, and DTRC Work Unit 1802-650.

## INTRODUCTION

Over the years vortex breakdown has played an increasing role in vortex control: Vortex stabilization in modern aircraft and gas mixing in combustion systems are two examples.<sup>1,2</sup> Ships and their appendages are surrounded by vortices, many of which are undesirable. Here too, vortex breakdown can be useful in vortex control. This paper discusses certain aspects of axisymmetric vortex breakdown as used in vortex control and the associated difficulties of defining vortex breakdown.

The commonly accepted phenomenological definition of vortex breakdown may be phrased in the form given by Faler and Leibovich:<sup>3</sup> ... the development of a stagnation point on the axis, followed by a region of reversed axial flow encapsulated by a greatly swollen stream surface, or in the more general form as expressed by Benjamin<sup>4</sup> as the abrupt and drastic change of structure which sometimes occurs in a swirling flow. Retardation of the axial velocity component can be achieved above a certain swirl parameter through axial pressure increase in the form of diverging streamlines, continuously or abruptly, or through jets or obstacles in the vortex core (Fig. 1). The occurrence of a stagnation point on the axis results either in axisymmetric vortex breakdown in the form of a "bubble", with possible subsequent disintegration, or in nonaxisymmetric vortex breakdown in the form of a spiraling vortex filament caused by instability. The flow fields in both forms can be either laminar or turbulent. In the turbulent case a higher degree of turbulence occurs after the bubble or spiral appears. Disintegration does not exclude partial swirl recovery as seen in Fig. 2a taken from Lugt's PhD thesis.<sup>5</sup> Recent reviews of the various theories

of vortex breakdown are given by Wedemeyer<sup>6</sup>, Leibovich<sup>7</sup>, and Escudier et al.<sup>8</sup> These reviews include discussions on the link of vortex breakdown to a supercritical state (that is, the existence of stationary waves as a prerequisite for vortex breakdown), the role of instability, and the influence of vorticity on vortex breakdown.

The term "vortex breakdown" or "vortex burst", dating back to about 1960,\* is justified as long as the vortex filament disintegrates. This terminology reflects the view that vortex breakdown is essentially an unstable, nonaxisymmetric, and time-dependent phenomenon which may be preceded by an almost axisymmetric bubble. A quotation from Leibovich<sup>9</sup> (p. 51) reads: ... *flow inside the bubble form is not axially symmetric, and azimuthal asymmetry seems to be characteristic of the bubble as well as the spiral form of breakdown.* Earlier studies which relied heavily on the axisymmetric flow model *may not be appropriate*, to quote Leibovich (p. 52) again.

This opinion is not generally shared. Others, Escudier and Keller,<sup>10</sup> for example, advocate the opposite point of view, that vortex breakdown is essentially an axisymmetric flow phenomenon and asymmetry is not essential. Here, opinions are divided on the role of instability. Some researchers still regard instability as an essential ingredient of vortex breakdown, some do not.<sup>6,11</sup>

Numerical results for axisymmetric, steady vortex breakdown, which do not display disintegration or spiraling vortex breakdown downstream of the bubble,<sup>12-14</sup> were viewed with suspicion as indicating either possibly unstable flows,<sup>7</sup> as in pipe or wing-tip flows, or questioned as to whether they indicated vortex breakdown at all,<sup>9</sup> as in container flow. The first argument is valid, depending on the viscous effects, but the second argument is not since axisymmetric and steady vortex breakdown conforms with the above-cited definitions of vortex breakdown.

These definitions do not stipulate that the flow past the axisymmetric bubble must disintegrate or become turbulent. Recent experimental and computational studies<sup>15-17</sup> of flow in containers demonstrated that axisymmetric vortex breakdown is a stable flow configuration in a certain parameter range without downstream disintegration, and the transition from a flow without a stagnation point on the axis to one with a stagnation point is smooth in the sense that, when the parameters are changed, the transition is continuous. Thus, instability does not account for the occurrence of axisymmetric vortex breakdown and is not inevitable behind the bubble. This view is contrary to the one presented in Ref. 15, in which the notation "stability limits" is used. In container flow - compared to pipe and wing-tip flows - a higher level of stability exists, because the recirculation of the fluid

---

\* In waterspouts, the term "vortex burst" was used much earlier. In fact, meteorologists must be given credit for having discovered the phenomenon of vortex breakdown. See the forthcoming paper on this subject by the senior author.

and the geometry (and thus the greater effect of viscosity) keep the fluid flow completely stable and steady. The closed container situation also has natural, unambiguous wall boundary conditions and parameters in contrast to the pipe or outer flows for which assumptions of the velocity profiles with corresponding parameters must be made. Even in these cases, stable axisymmetric flows have been observed, as the ducted exit flows of burners<sup>2</sup> demonstrate. It is worth mentioning here that turbulent axisymmetric bubbles exist,<sup>2,10</sup> indicating how stable these flows are against non-axisymmetric disturbances.

For non-axisymmetric vortex burst, instability is essential to account for the symmetry breaking from an axisymmetric upstream flow.

The term "vortex breakdown" or "vortex burst", then, is improper when no disintegration takes place as in the axisymmetric container flow (it is too late now, of course, to change the wording). This is probably the reason for the confusion in the literature on the labelling of "vortex breakdown" versus "recirculating region" of the axisymmetric type (Fig. 1). For instance, in the Gupta et al. book on swirling motion,<sup>2</sup> the recirculating region behind the exit nozzle of burners is not considered vortex breakdown (at least the term is not used, and reference is made to a "similarity" between the two terms) although the region fulfills the criterion for vortex breakdown: the bubble is completely surrounded by fluid with two axial stagnation points (Fig. 1c). Vortex breakdown as such is regarded in that book, p. 187, as an instability problem. Other publications<sup>18,19</sup> treat the recirculation region clearly as vortex breakdown. This association has also been made for bubbles in rotating cylindrical cavity flows.<sup>20</sup>

The confusion is compounded when there is no axial stagnation point, as might happen for strong bubbles which become annular. This situation will be demonstrated in this paper. The lack of an axial stagnation point was also observed by Phillips<sup>21</sup> in non-axisymmetric vortex breakdown when the spiral disturbance spins in the direction opposite to the vortical rotation.

If a rod is placed along the vortex axis, the phenomenon of vortex breakdown can still occur. Examples are furnished in Fig. 2b for the case of turbulent spiral vortex breakdown<sup>5</sup> and by Escudier and Keller<sup>10</sup> for multiple bubble-type breakdowns. On the other hand, this conclusion that separation bubbles are considered as vortex breakdown may not be reached for bubbles behind the centerbody of an exit nozzle (Fig. 1d). A gray area of vagueness exists.

This vagueness is supported if one considers that the placement of an obstacle on the vortex axis transforms the vortex-breakdown problem to a special case of a Taylor-Proudman problem,<sup>22,23</sup> that is, the case of the axis of rotation parallel to the fluid flow. The separation zones in front of and behind the obstacle can be interpreted as remnants of a Taylor-Proudman column that would extend toward infinity for vanishing viscosity and would be demarcated by two characteristics. Although this column owes its existence to the wave property of the rotating fluid, it must be distinguished from vortex breakdown.

The boundary of the Taylor-Proudman column, degenerated to finite separation regions in the front and rear of the obstacle through viscosity, is determined by the outer dimensions of the body. Vortex breakdown, on the other hand, is a wave phenomenon with waves perpendicular to the axis of rotation. Thus, the separation region in Fig. 1d must be considered a remnant of a Taylor-Proudman column, whereas the flow patterns in Fig. 2b and those described by Escudier and Keller<sup>10</sup> can be attributed to vortex breakdown. The question of whether any separation region on the obstacle can be related to vortex breakdown, however, remains unanswered.

The present study on this subject is restricted to an idealized wing-tip vortex as a special kind of axisymmetric flow, with and without obstacles in the vortex core. These obstacles are intended as a control device to induce vortex breakdown. The restriction of axisymmetry is used in the present study. Stability must, therefore, be verified a posteriori elsewhere. An extension of this study to three-dimensional flows that will address this question will be reported in a forthcoming article.

#### DESCRIPTION OF THE FLOW MODEL AND NUMERICAL ALGORITHM

An axisymmetric laminar swirling motion is assumed that is described by the Navier-Stokes equations for a steady, incompressible fluid flow in cylindrical polar coordinates  $r, \varphi, z$  with the corresponding velocity components  $u, v, w$ . Axisymmetry requires  $\partial/\partial\varphi \equiv 0$ . Then, the continuity and the Navier-Stokes equations reduce to

$$\frac{\partial u}{\partial r} + \frac{u}{r} + \frac{\partial w}{\partial z} = 0, \quad (1)$$

$$u \frac{\partial u}{\partial r} + w \frac{\partial u}{\partial z} - \frac{v^2}{r} = - \frac{\partial p}{\partial r} + \frac{1}{Re} \left( \frac{\partial^2 u}{\partial r^2} + \frac{1}{r} \frac{\partial u}{\partial r} - \frac{u}{r^2} + \frac{\partial^2 u}{\partial z^2} \right), \quad (2)$$

$$u \frac{\partial v}{\partial r} + w \frac{\partial v}{\partial z} + \frac{uv}{r} = \frac{1}{Re} \left( \frac{\partial^2 v}{\partial r^2} + \frac{1}{r} \frac{\partial v}{\partial r} - \frac{v}{r^2} + \frac{\partial^2 v}{\partial z^2} \right), \quad (3)$$

$$u \frac{\partial w}{\partial r} + w \frac{\partial w}{\partial z} = - \frac{\partial p}{\partial z} + \frac{1}{Re} \left( \frac{\partial^2 w}{\partial r^2} + \frac{1}{r} \frac{\partial w}{\partial r} + \frac{\partial^2 w}{\partial z^2} \right). \quad (4)$$

The independent and dependent quantities have been made dimensionless by the core radius  $r_c^*$ , where the (dimensional) tangential velocity has its maximum value  $v^* = v_{\max}^*$ , and  $v_{\max}^*$  as characteristic length and velocity, respectively. The Reynolds number is given by  $Re = r_c^* v_{\max}^* / \nu$ , with  $\nu$  the kinematic viscosity.

The problem is completely defined if the boundary conditions of the infinite flow field are specified. This field is reduced in the computational domain to a finite circular cylinder of radius  $r = R$  and length  $z = L$ . At the

wall of the cylinder  $r = R$  the velocity components are  $u = 0$ ,  $v = v(R) \ll 1$ ,  $w = W/v^*_{\max}$ , and the pressure is  $p_\infty$ . At the axis  $r = 0$ , the conditions are  $u = v = 0$ ,  $\partial w/\partial r = 0$ , and  $\partial p/\partial r = 0$ . In the entrance area  $z = 0$ ,  $0 \leq r \leq R$ , the boundary conditions are given by the following class of velocity profiles that model a wing-tip vortex:<sup>24</sup>

$$u(r) = 0,$$

$$v(r) = \frac{1}{r} \frac{1 - e^{-ar^2}}{1 - e^{-a}}, \quad (5)$$

$$w(r) = \frac{W}{v^*_{\max}} = \text{const},$$

and by the pressure gradient:

$$\frac{\partial p}{\partial z} = 0. \quad (6)$$

The exit conditions at  $z = L$ ,  $0 \leq r \leq R$  are

$$\frac{\partial F}{\partial z} = 0 \quad (7)$$

for all variables  $F$ .

According to Eq. 5 the core radius is  $r = r_c = 1.122/\sqrt{a}$ . The constant of the axial velocity component in Eq. 5 can also be interpreted as the reciprocal of the swirl parameter  $S = v^*_{\max}/W$ . The parameters describing the problem are, thus,  $Re$ ,  $S$ , and  $a$ .

If an obstacle is included, either on the axis or around the axis, the boundary of this obstacle is determined by the vanishing normal velocity component. In addition the nonslip condition must be considered. A thin rod, a nozzle, and a sphere were chosen as obstacles.

For the wing-tip vortex Squire<sup>25</sup> derived the following criterion for vortex breakdown (or to be more precise, a criterion for the existence of infinitesimal stationary waves):

$$S \geq 1. \quad (8)$$

More recently, an empirical criterion was found by Spall et al.<sup>24</sup> which is independent of the Reynolds number for values larger than 100S:

$$S \geq 0.88. \quad (9)$$

In the paper by Spall et al.<sup>24</sup> the Rossby number  $Ro = W/\Omega r_c^*$  and the Reynolds number  $Re = Wr_c^*/\nu$  are used instead of  $S$  and  $Re$ .  $\Omega$  is the angular velocity of the vortex at  $r = 0$ . These parameters are related to each other by

$$Ro = \frac{W}{\Omega r_c^*} = \frac{v_{\max}^*}{\Omega r_c^*} \cdot \frac{W}{v_{\max}^*} = \frac{0.569}{S} , \quad (10)$$

$$Re = \frac{Re}{S} . \quad (11)$$

The elliptic boundary-value problem of Eqs. 1 through 7 is a well-posed problem, and solutions represent realistic flows. It is similar to that described by Grabowski and Berger<sup>13</sup> and is solved in the following way: A pseudo-compressibility technique developed by Chorin<sup>26</sup> has been used with a pseudo-time term added to the continuity equation. This makes the Navier-Stokes equations hyperbolic in time and permits the application of discretization methods for compressible fluids. The nonlinear inertial terms are replaced by a third-order upwind differenced TVD (Total Variation Diminishing) scheme developed by Chakravarthy et al.,<sup>27,28</sup> whereas the linear viscous terms are discretized by central difference operators. Details of the solution algorithm can be found in Gorski.<sup>29</sup>

The grid is displayed in such a way that, in the area of high resolution  $0 \leq r \leq R$ ,  $0 \leq z \leq 15$ , the grid points are evenly distributed, whereas outside this area the grid is stretched exponentially (Fig. 3). The total number of grid points is  $80 \times 70$  in the  $r$ - and  $z$ - directions, with  $R = 19$  and  $L = 60$ . Figs. 4 through 6 show the grids with rod, nozzle, and sphere as built-in obstacles.

The accuracy of the computer program has been checked with results of Grabowski and Berger<sup>13</sup> and Lugt and Abboud<sup>17</sup> whose data were obtained by completely different numerical techniques based on the streamfunction-vorticity formulation. The agreement in all cases is good. Moreover, Lugt and Abboud's streamline patterns concur well with Escudier's photographs.<sup>15</sup>

The results of this study are presented in the form of streamlines and  $w$ -values along the axis of rotation.

## RESULTS

Numerical data have been obtained for flows with and without obstacles and for the two Reynolds numbers 500 and 2500. The constant  $a$  is assumed to be  $a = 1$  throughout.

### WITHOUT OBSTACLES

For  $Re = 500$  the streamline patterns and  $w$ -components for the sequence of cases  $S = 0.80, 0.82, 0.83, 0.85, 0.87$ , and  $1.05$  are shown in Figs. 7 through 13.

The first occurrence of a bubble, that is, vortex breakdown, happens between  $0.80 < S < 0.82$ . This agrees fairly well with the criterion of Eq. 9 if one considers the large scattering of data from which that criterion was derived. The result, however, agrees well with Grabowski and Berger's output.<sup>13</sup>

With increasing  $S$  the bubble thickens and migrates upstream (Fig. 9). Simultaneously, the streamlines near the axis widen farther downstream which, for  $S = 0.85$ , results in a second bubble (Fig. 10). With continued increase of  $S$  the two bubbles enlarge (Fig. 11), and the second bubble takes the form of a "cucumber", indicating the embryonic state of a third bubble<sup>17</sup>. In Fig. 12 only part of the flow field is displayed. The internal structure of the first bubble agrees with that found in the literature.<sup>14</sup>

The axial velocity on the centerline  $r = 0$  complements the above scenario. Figs. 7 through 13 confirm also the large gradient of  $w$  immediately behind the entrance section  $z = 0$ . Fig. 13 reveals that the first bubble does not have axial stagnation points, that is, the bubble is actually a rotating vortex ring with a nonvanishing axial flow component. Indications of this phenomenon are observed in other publications.<sup>2,18</sup> This means that the definition of vortex breakdown which requires the existence of an axial stagnation point must be phrased in a more general form, for instance, the form by Benjamin given above.

The results for  $Re = 2500$  are very similar to those for  $Re = 500$  except that the bubble first appears at a slightly higher value of  $S$ , that is, at  $S = 0.85$  (Fig. 14).

## WITH OBSTACLES

In the first series of numerical experiments, with obstacles inside the vortex core, rods of length 5 and thicknesses 0.1 and 0.2 with conical endings (Fig. 4) were placed with their front at  $r = 4.5$ . The Reynolds number and swirl parameters chosen were  $Re = 500$  and  $S = 0.80$  and 0.82 (Figs. 15 through 17). The vortex flow around the thin rod shows no sign of flow separation, whereas the thick rod exhibits separation toward the mid-section of the body (Fig. 16). Although this ring-shaped separation bubble resembles the bubbles observed by Escudier and Keller<sup>10</sup> for much higher Reynolds numbers, one may hesitate to call this separation vortex breakdown and may attribute it to normal flow separation due to friction. This influence of viscosity is clearly noticeable in the flow situation of Fig. 17, which does not reveal a bubble, while the flow without a rod does (Fig. 8). Apparently viscous effects around the rod suppress the occurrence of the vortex breakdown bubble, contrary to what experiments with high Reynolds numbers show, that is, a rod induces vortex breakdown in an otherwise stable vortex.<sup>30</sup>

One expects the appearance of separation regions in the front and rear of the obstacle to be remnants of Taylor-Proudman columns. However, the demarcation between vortex breakdown and Taylor-Proudman column is not well defined.

In the second series a conical ring ("nozzle") was placed on the axis of the vortex, with the larger opening upstream. Again, the Reynolds number and swirl parameters were chosen to be  $Re = 500$ ,  $S = 0.80$  and  $S = 0.82$  (Figs. 18 and 19). For  $S = 0.80$ , for which the flow without an obstacle does not have a bubble, the streamlines diverge ahead of the nozzle without

forming a bubble. Directly at the nozzle entry two counter-rotating vortex rings appear, and inside the nozzle the streamlines again diverge (Fig. 18). The situation is quite different for  $S = 0.82$ . The streamlines ahead of the nozzle now diverge so strongly that the  $w$ -component almost reaches zero in Fig. 19. The counter-rotating vortices have been replaced by wavy motions. The (almost) occurrence of vortex breakdown in front of the nozzle agrees qualitatively with experiments for high Reynolds numbers that show spiral vortex breakdown in front of the nozzle.<sup>30</sup>

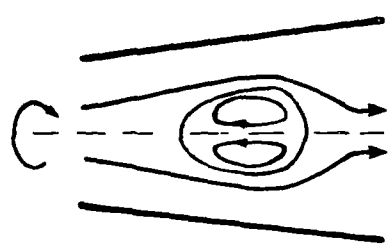
If the nozzle is reversed, that is, the smaller opening is upstream, the numerical calculations do not converge for  $Re = 500, S = 0.80$ . It is suspected that a steady-state solution does not exist for this special flow situation.

In the final series a sphere was introduced into the axis of rotation. This case is similar to those studied in context with the Taylor-Proudman column.<sup>22,23</sup> The surprising result is that, in addition to the front and rear separation regions at the sphere, vortex breakdown upstream of the sphere occurs, a phenomenon not observed in previous investigations (Fig. 20). The corresponding flow without a sphere exhibits no vortex breakdown (Fig. 7).

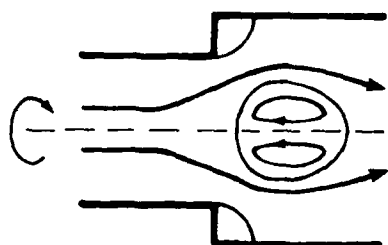
### CONCLUSIONS

The placement of obstacles into the core of vortices as a means of controlling them raises questions about the definition of vortex breakdown. Whereas it is generally agreed that steady-state, stable bubbles at the axis of the vortex constitute vortex breakdown, a dilemma exists when an obstacle distorts this picture. On one hand, photographs and numerical calculations reveal a clear situation of vortex breakdown (Fig. 2b); on the other hand, a separation region can be interpreted as a truncated Taylor-Proudman column. The following distinction is made: If the separation regions are in front and in the rear of the obstacles, they are considered remnants of Taylor-Proudman columns. If the separation regions are sidewise on the body, they may be attributed to vortex breakdown. Here, however, a certain vagueness remains on whether these separation regions might also be interpreted as simple viscous flow separation areas.

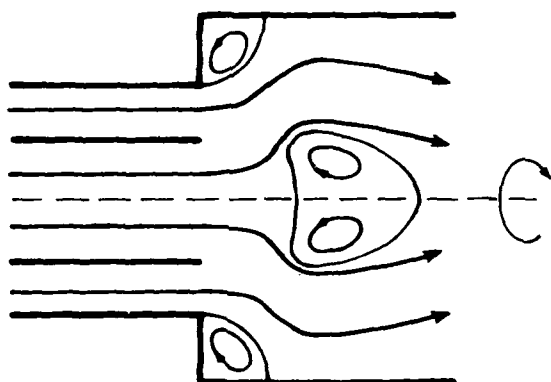
For the low Reynolds numbers chosen in this study, the introduction of a rod into the vortex core stabilizes the flow, contrary to the observation made for high Reynolds numbers. A nozzle with the larger cross-section upstream, however, can cause vortex breakdown in front of it. The same is true if a sphere is used.



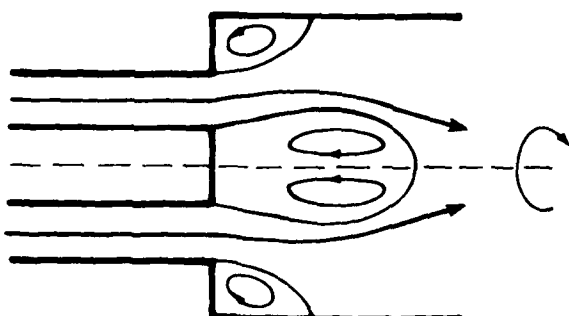
a



b



c



d

**Fig. 1.** Sketches of steady-state meridional streamlines of axisymmetric vortex-breakdown bubbles: (a) in a diverging tube, (b) at an abrupt enlargement of a tube, and (c) at the exit of an annular tube with two different velocities in ring and core of the tube. (d) The bubble behind the center body of the exit of the tube is not considered vortex breakdown.



a



b

**Fig. 2.** Spiral vortex breakdown in a turbulent swirling pipe flow behind an orifice made visible by a hollow-core cavitation of gas along the axis. (a) Without a rod. The Reynolds number is  $Re = 10^5$ , defined by the average axial velocity and the inner diameter of the pipe; and (b) with a rod at the axis. (Photographs from Ref. 5)

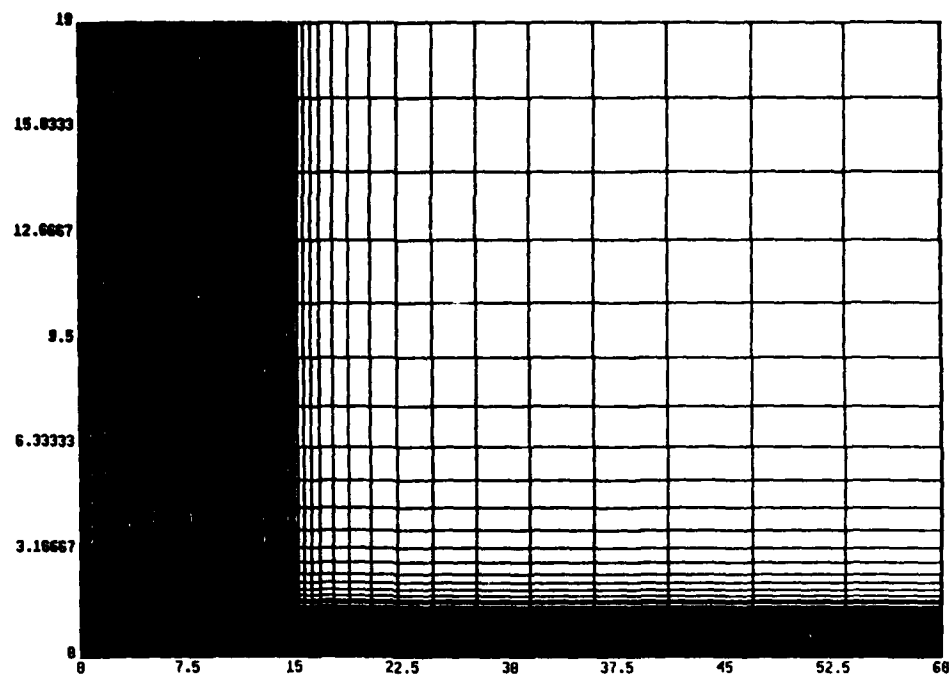


Fig. 3. Grid of the computational half-plane.

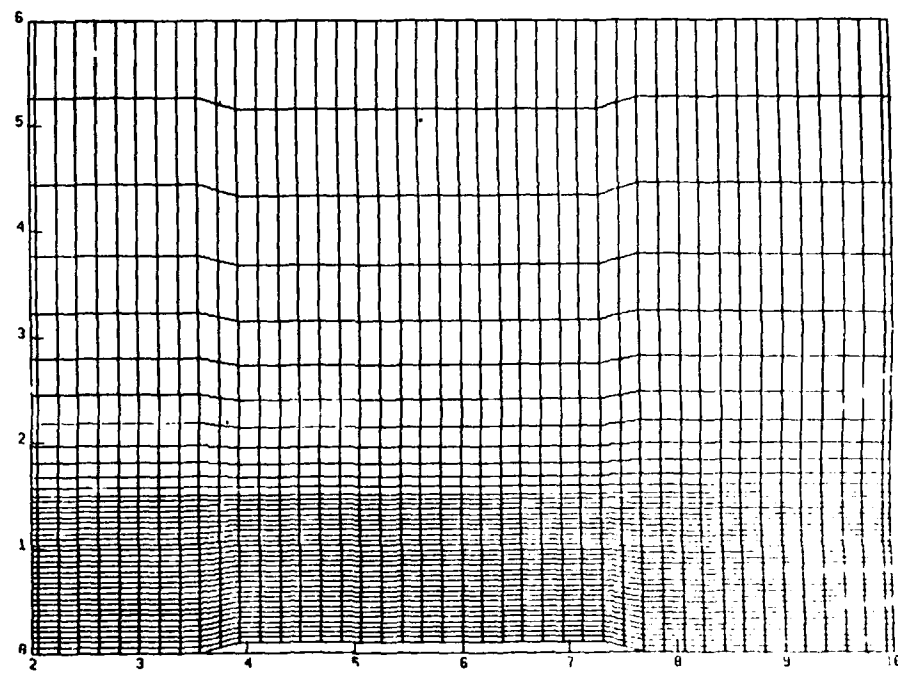


Fig. 4. Grid of the computational half-plane with a wavy boundary.

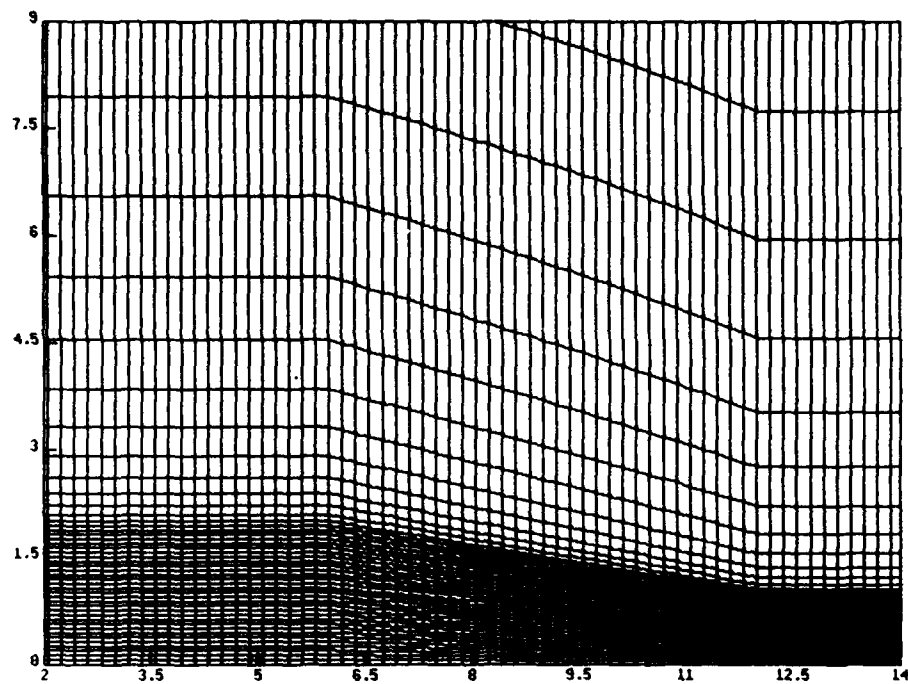


Fig. 5. Grid of the computational half-plane with a ring-shaped body at the axis "nozzle".

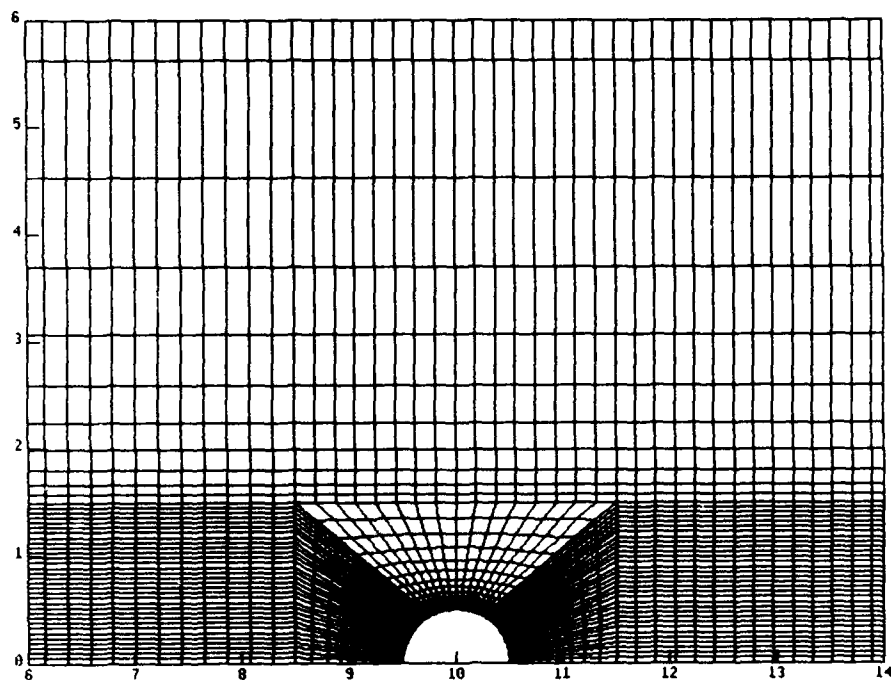
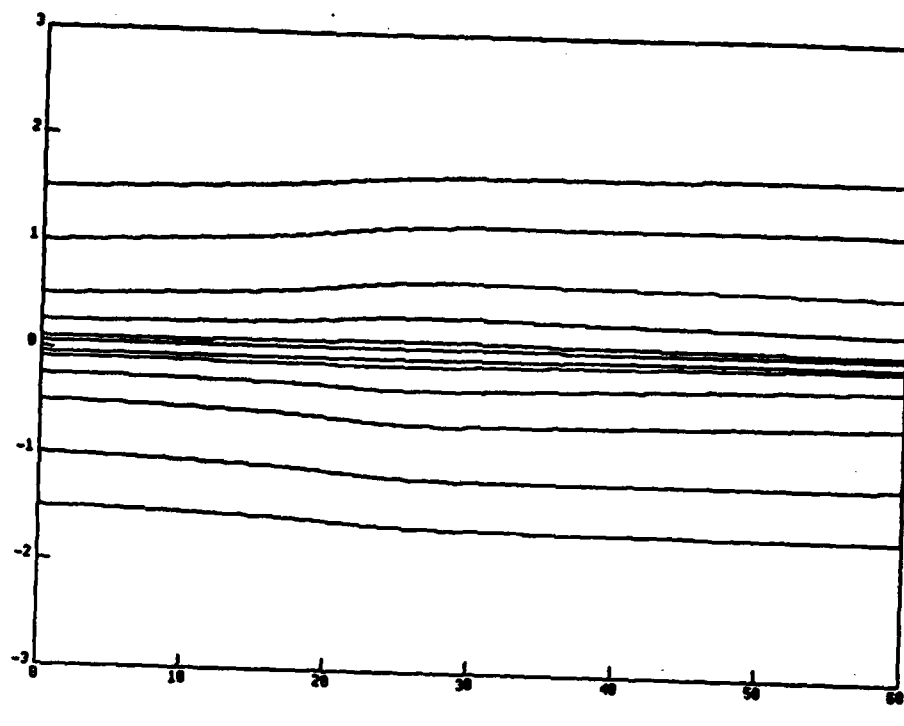
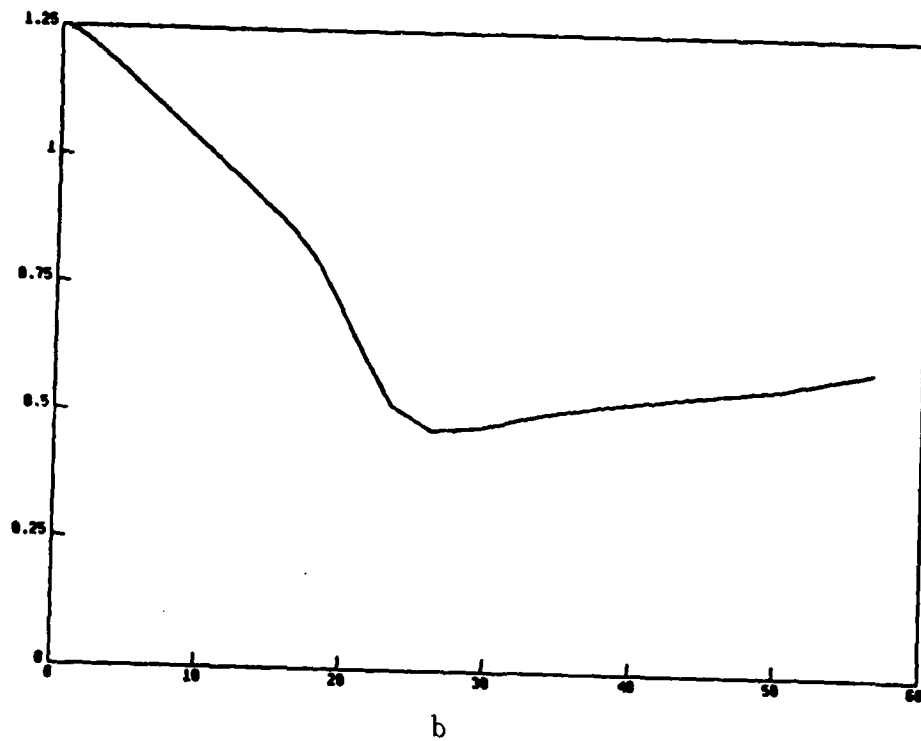


Fig. 6. Grid of the computational half-plane with a sphere at the axis.



a



b

Fig. 7. Flow field for  $Re = 500$ ,  $S = 0.80$ . (a) Meridional streamlines, and (b)  $w$ -component at the axis of rotation.

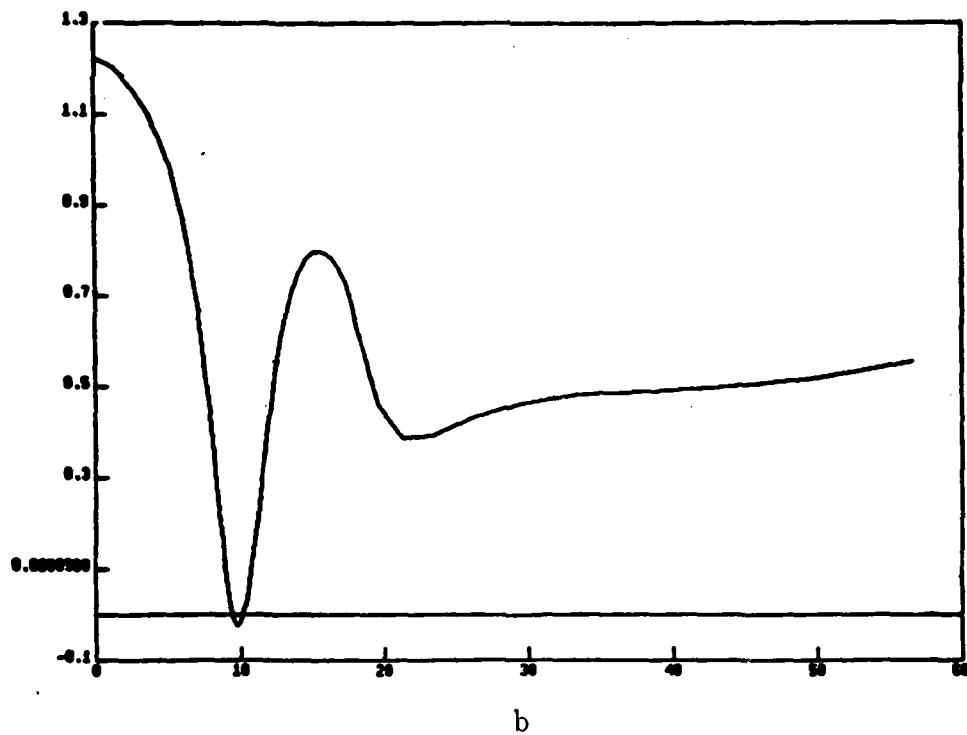
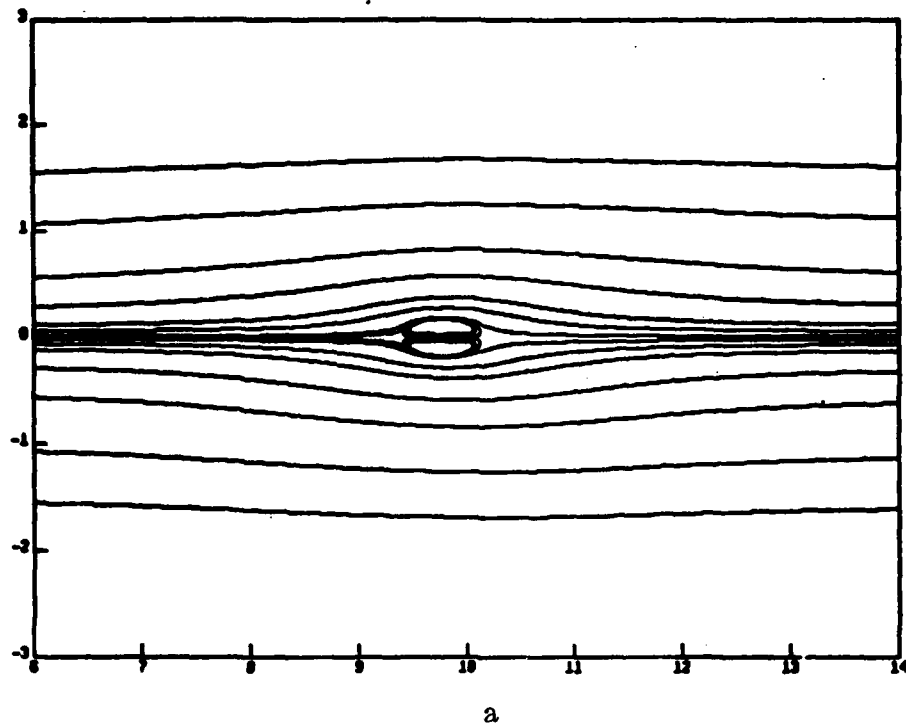
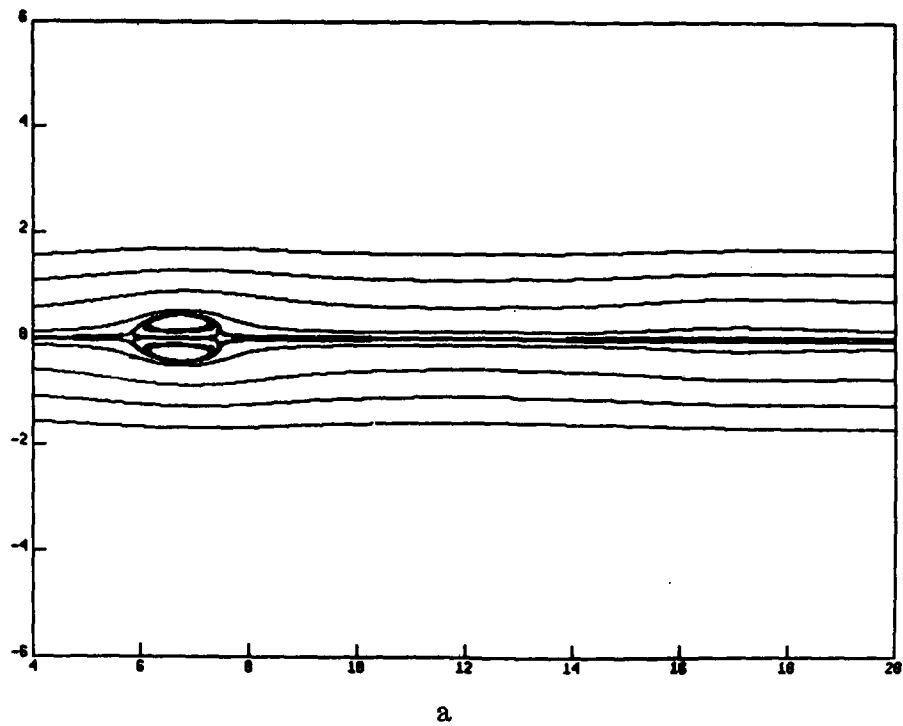
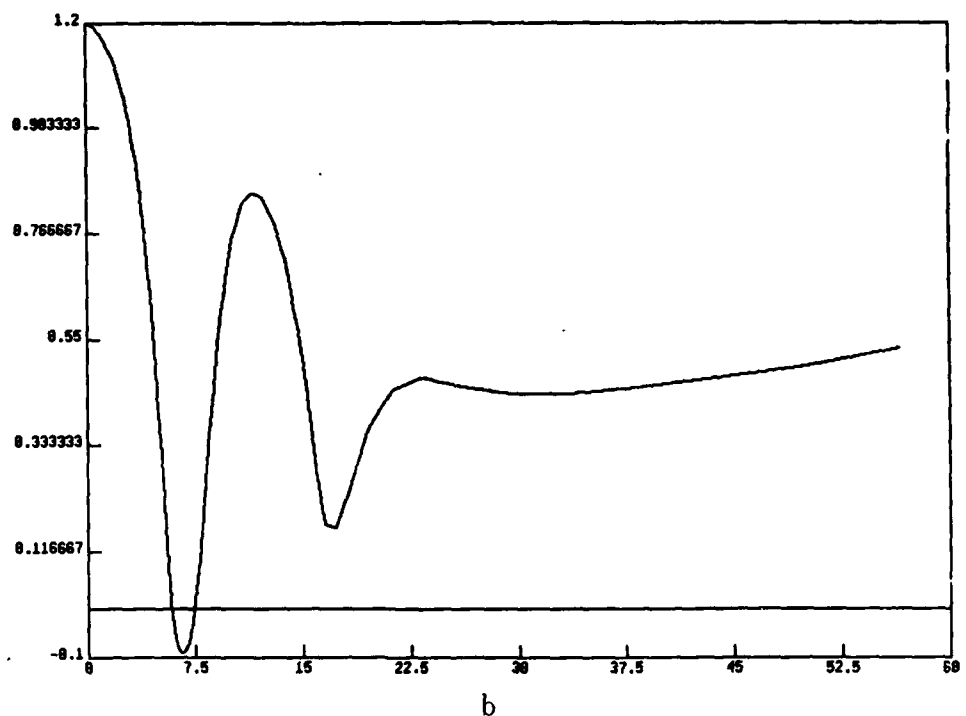


**Fig. 8.** Flow field for  $Re = 500$ ,  $S = 0.82$ . (a) Meridional streamlines, and (b)  $w$ -component at the axis of rotation.

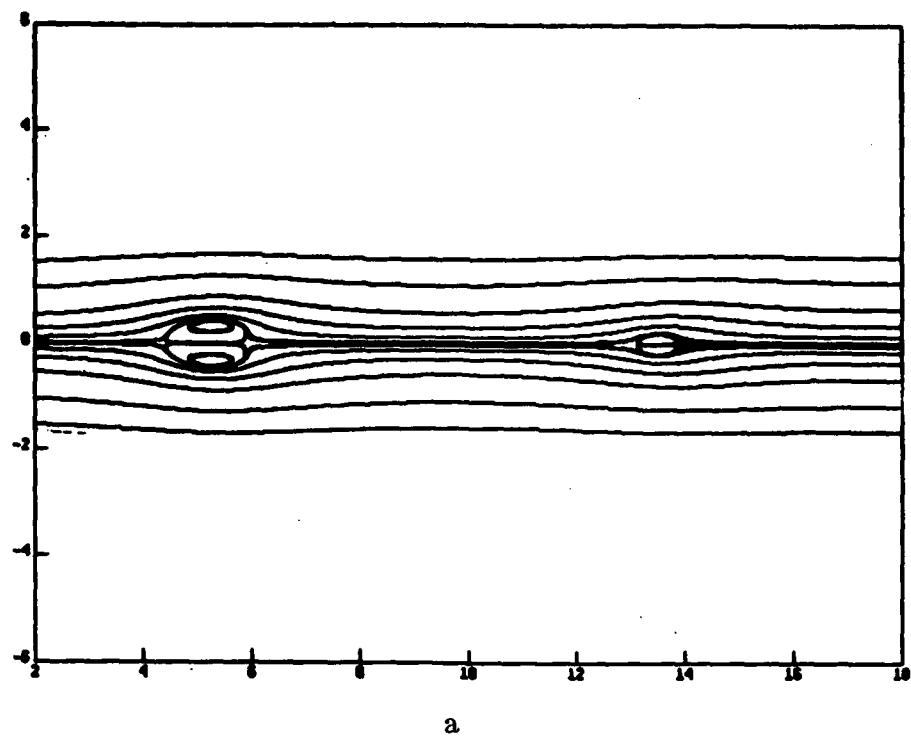


a

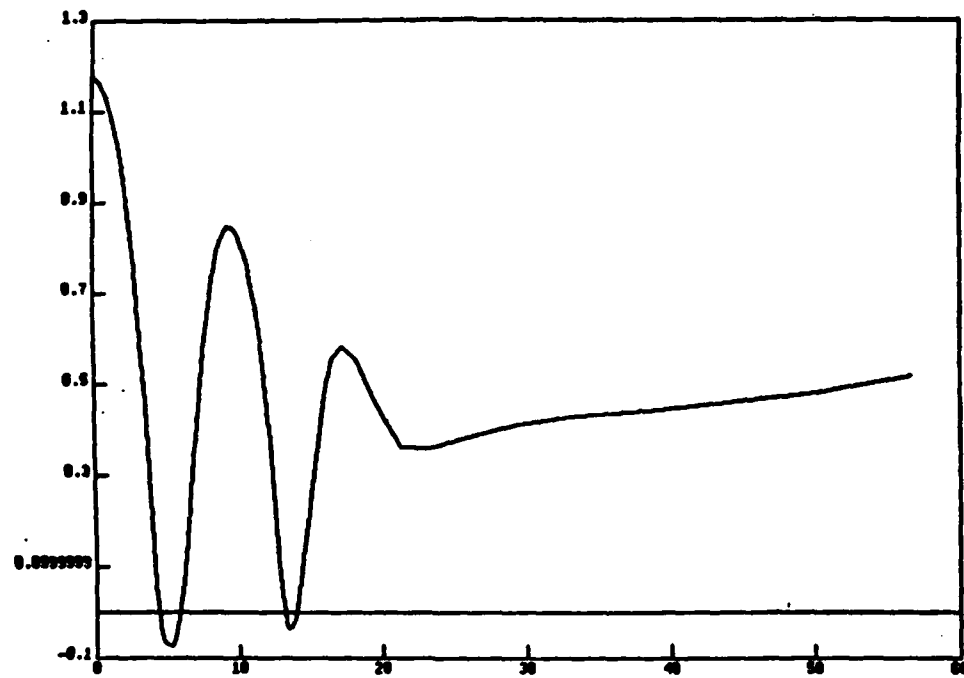


b

**Fig. 9.** Flow field for  $Re = 500$ ,  $S = 0.83$ . (a) Meridional streamlines, and (b)  $w$ -component at the axis of rotation.

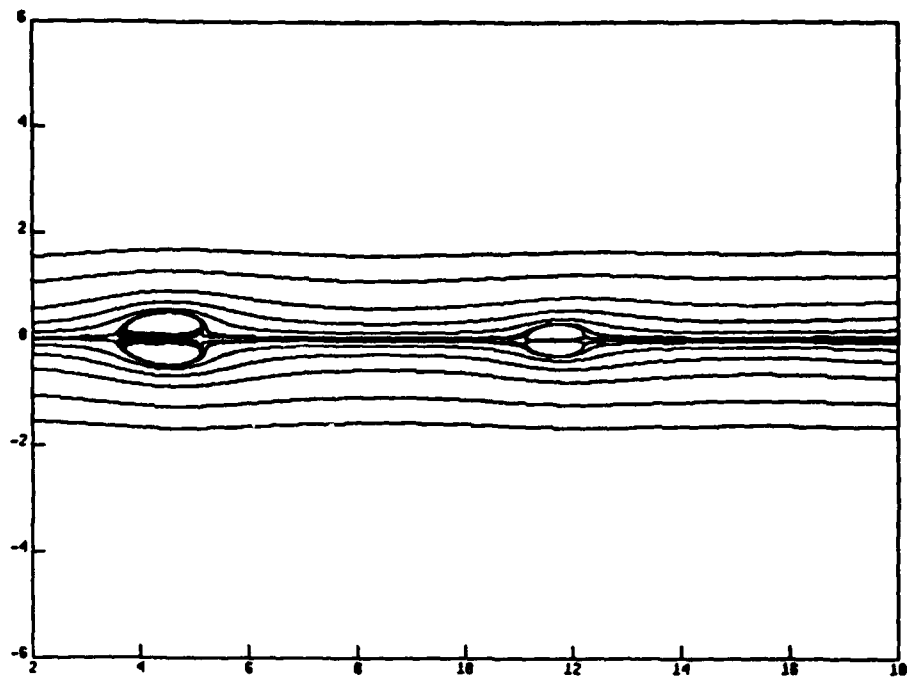


a

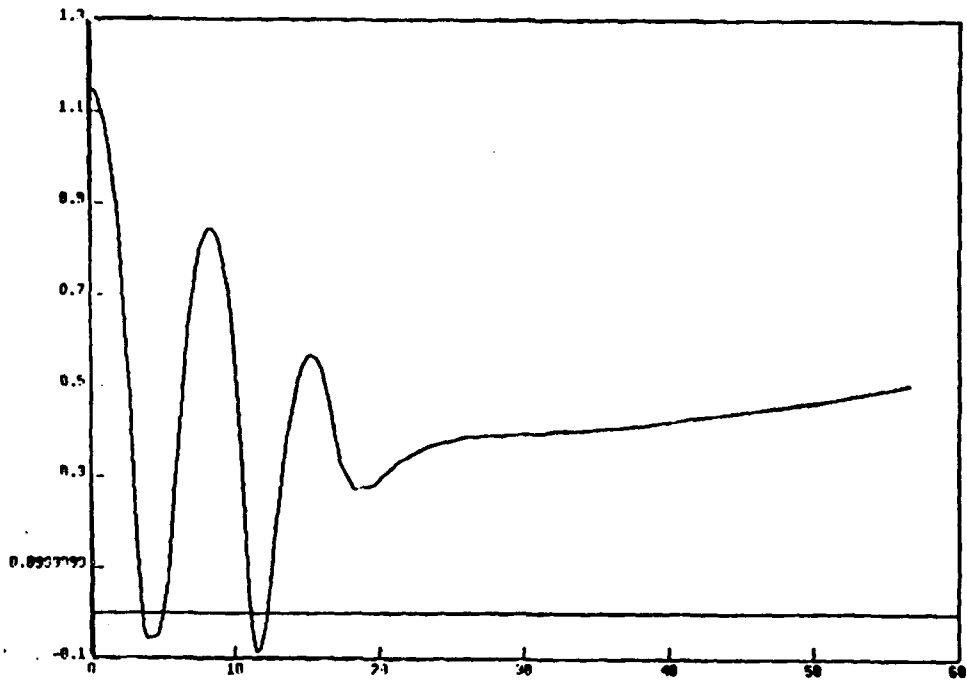


b

**Fig. 10.** Flow field for  $Re = 500$ ,  $S = 0.85$ . (a) Meridional streamlines, and (b)  $w$ -component at the axis of rotation.

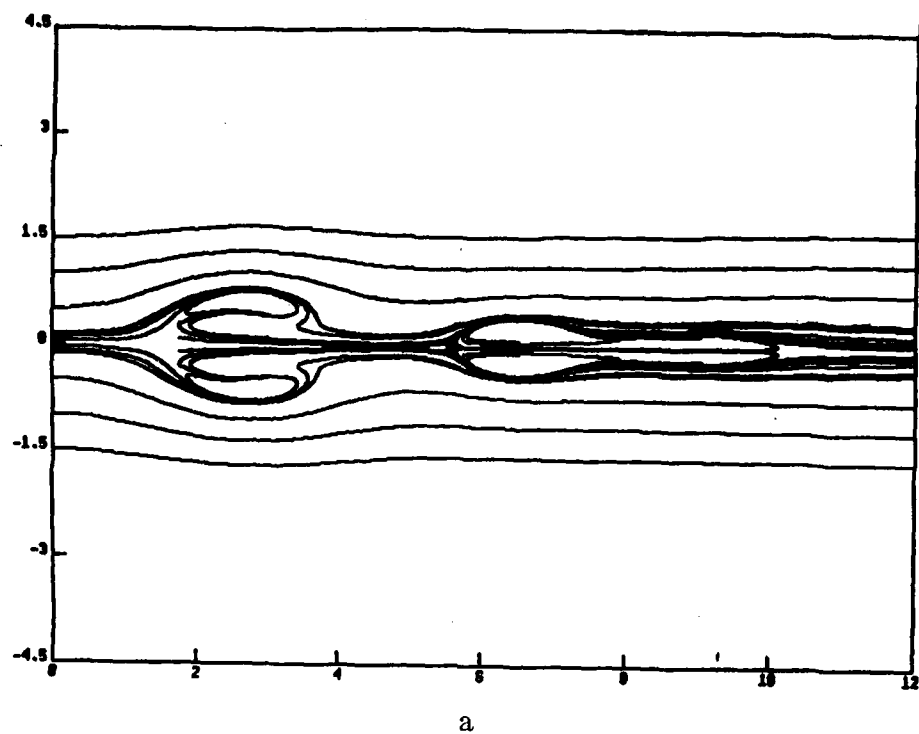


a

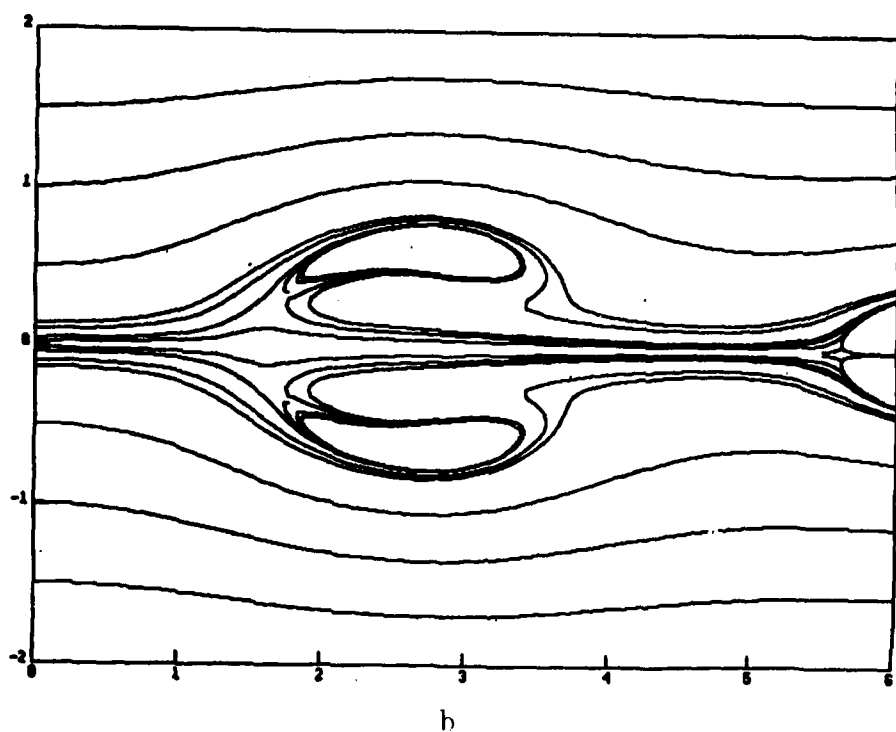


b

**Fig. 11.** Flow field for  $Re = 500$ ,  $S = 0.87$ . (a) Meridional streamlines, and (b)  $w$ -component at the axis of rotation.



a



b

**Fig. 12.** Flow field for  $Re = 500$ ,  $S = 1.05$ . (a) Meridional streamlines, and (b) enlarged section.

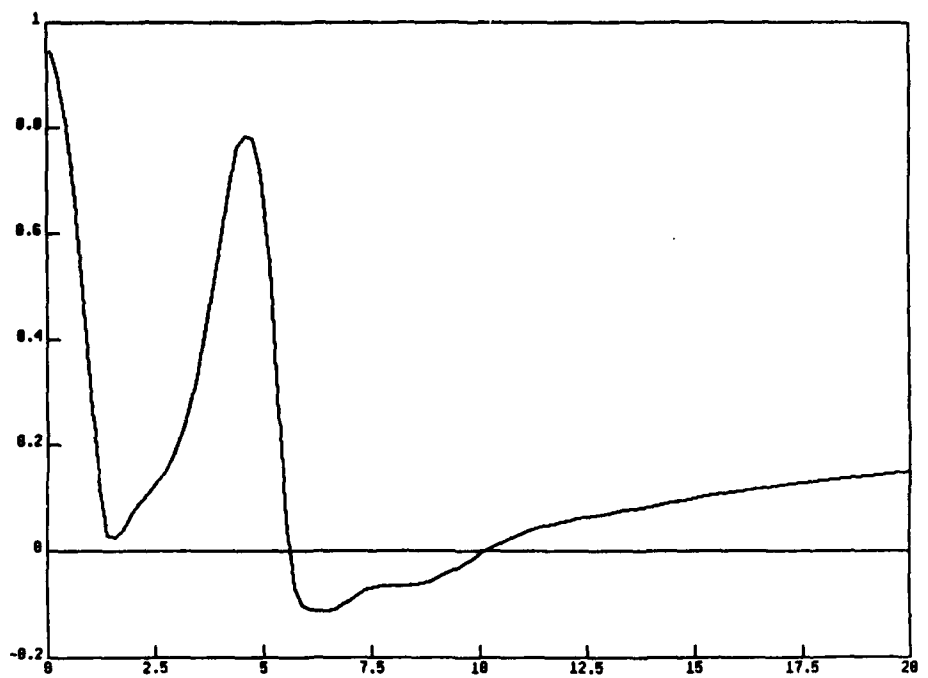
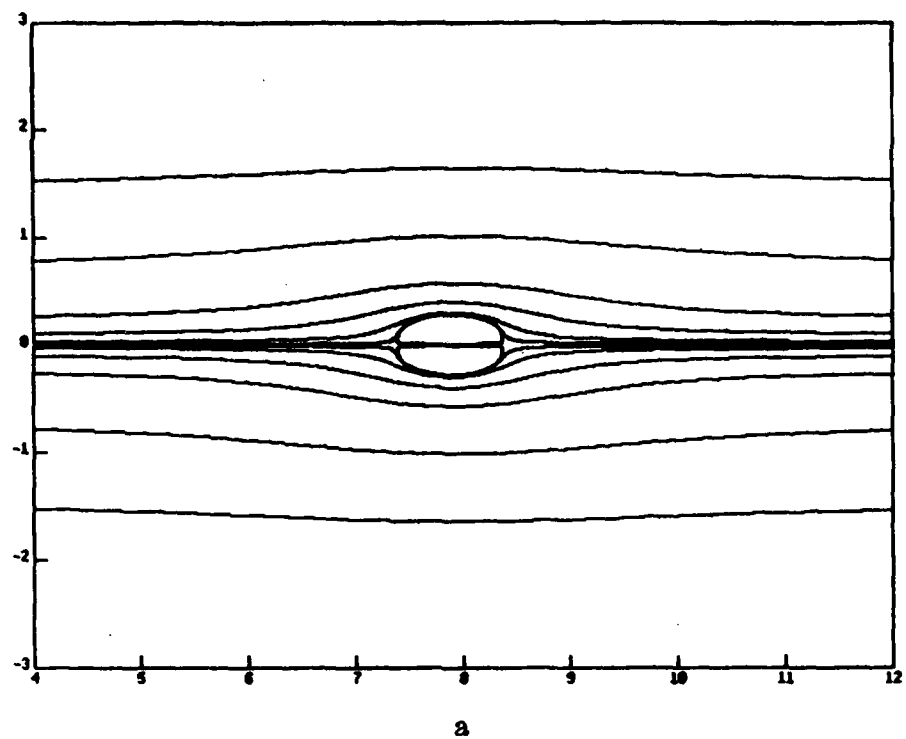
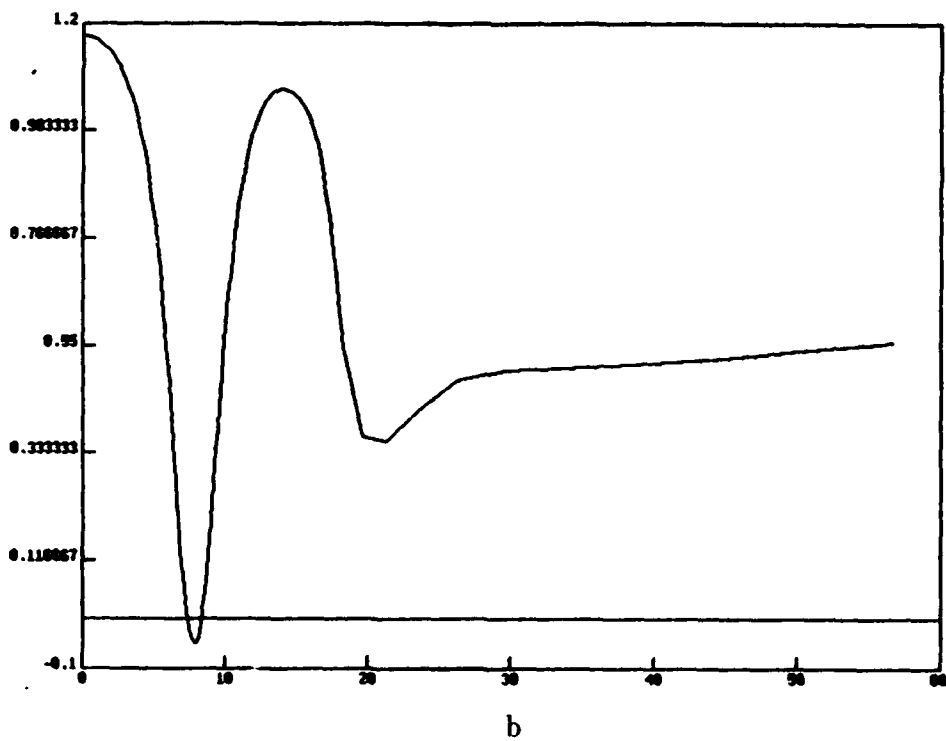


**Fig. 13.**  $w$ -component at the axis of rotation for  $Re = 500$ ,  $S = 1.05$ .



a



b

**Fig. 14.** Flow field for  $Re = 2500$ ,  $S = 0.85$ . (a) Meridional streamlines, and (b)  $w$ -component at the axis of rotation.

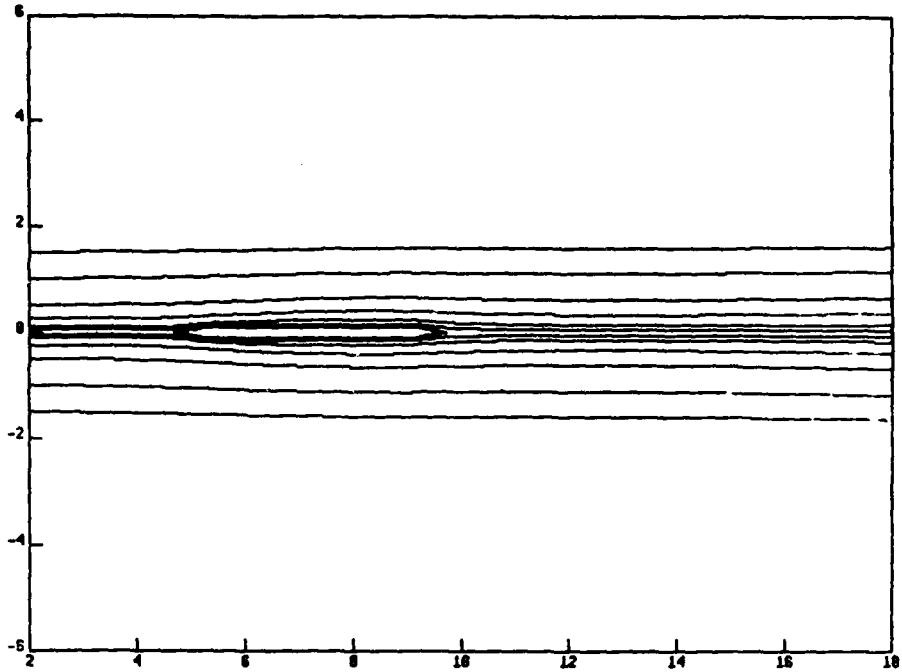


**Fig. 15.** Meridional streamlines for  $Re = 500$ ,  $S = 0.80$  with a rod,  $R_{st} = 0.1$ .

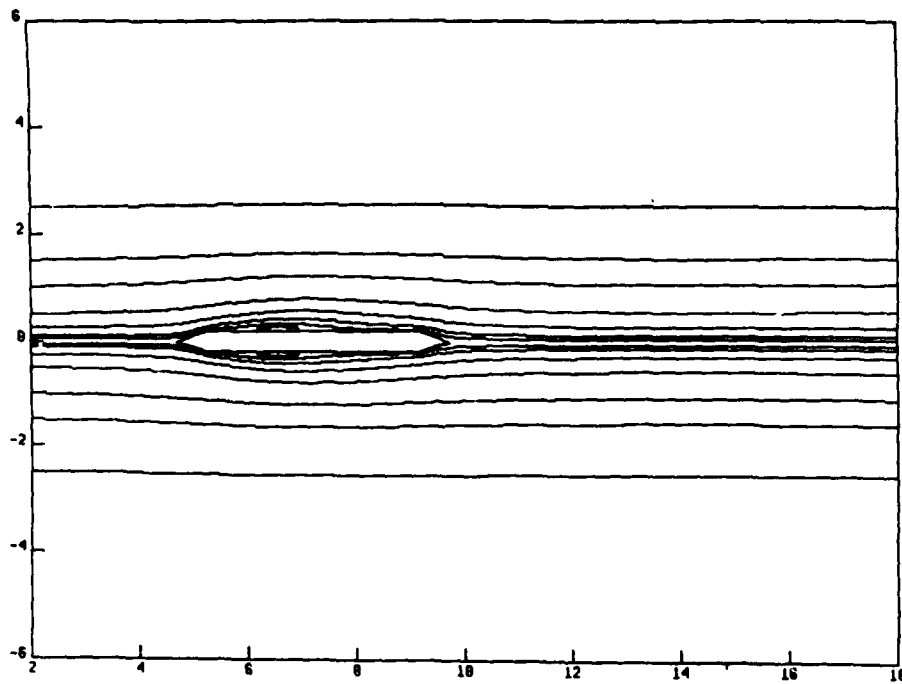


**Fig. 16.** Meridional streamlines for  $Re = 500$ ,  $S = 0.80$  with a rod,  $R_{st} = 0.2$ .

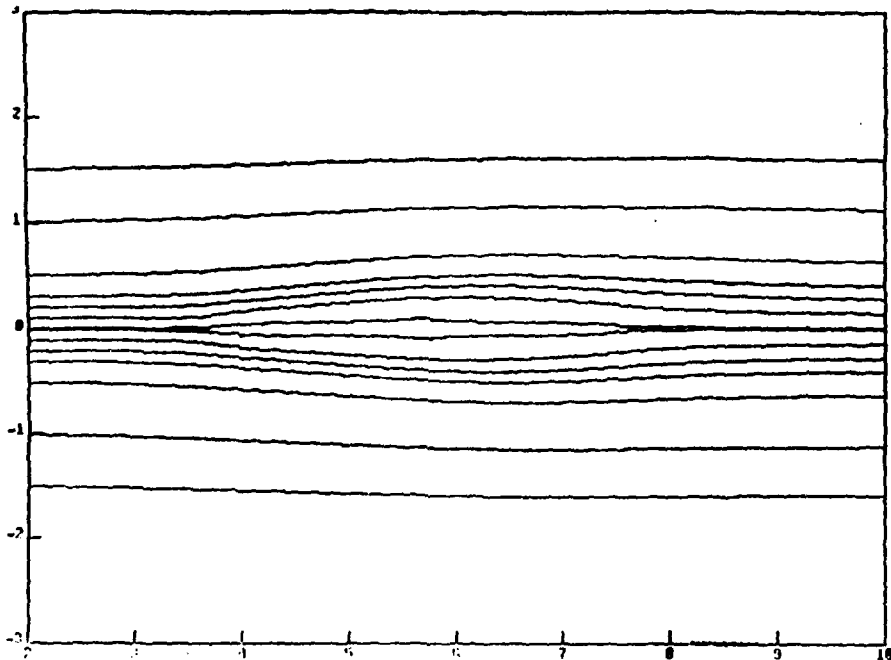
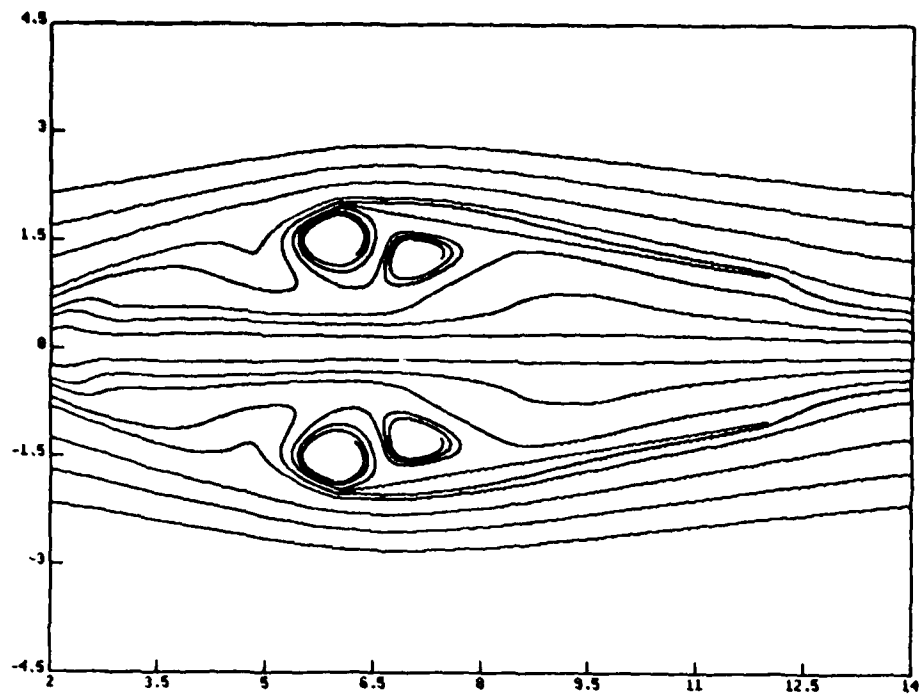
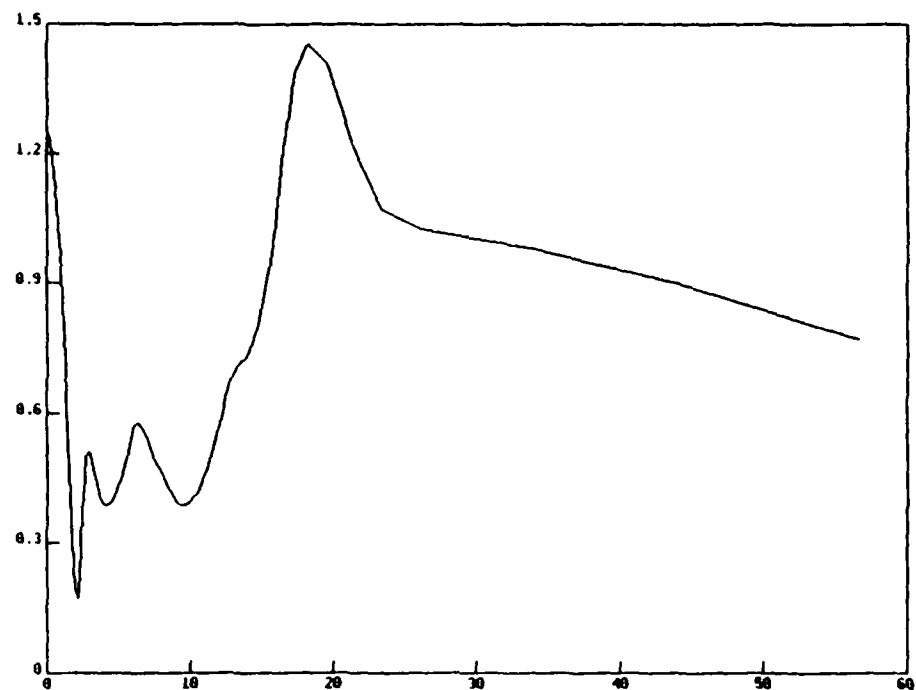


**Fig. 17.** Meridional streamlines for  $Re = 500$ ,  $S = 0.82$  with a rod,  $R_{st} = 0.1$ .

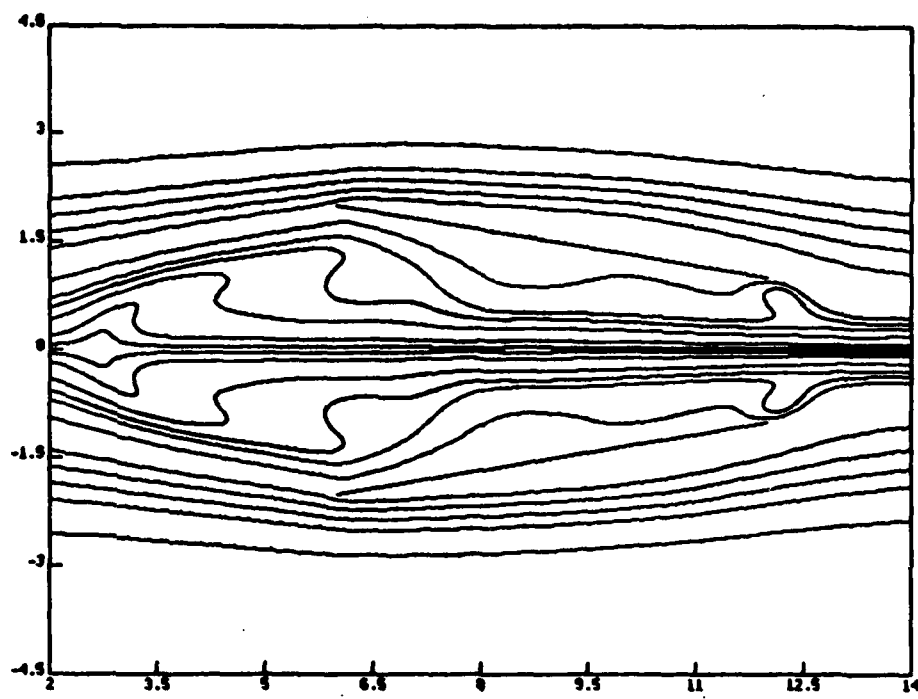


a

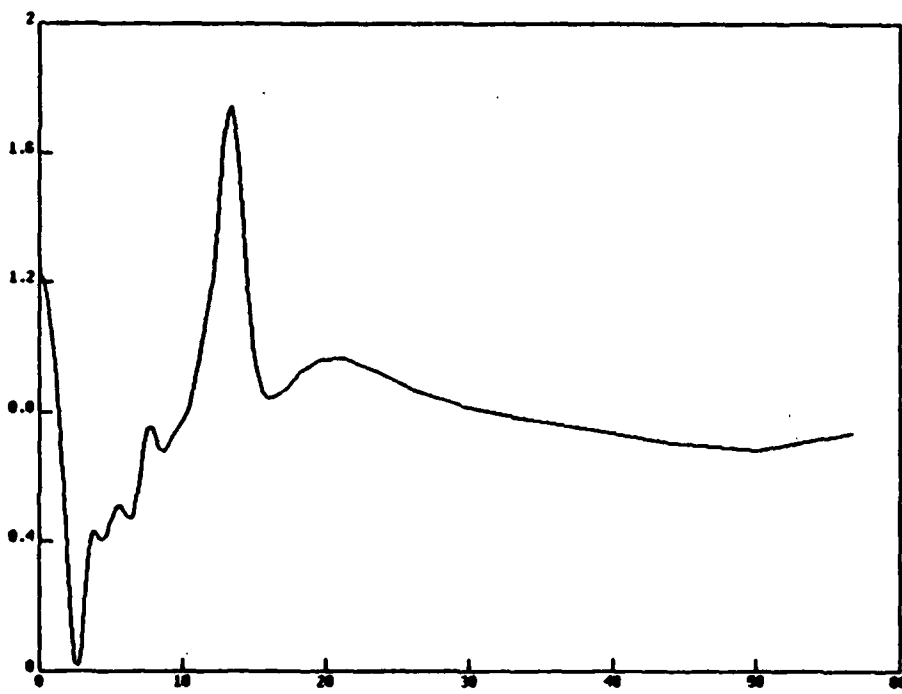


b

Fig. 18. Flow field for  $Re = 500$ ,  $S = 0.80$  with a nozzle. (a) Meridional streamlines, and (b)  $w$ -component at the axis of rotation.



a



b

**Fig. 19.** Flow field for  $Re = 500$ ,  $S = 0.82$  with a nozzle. (a) Meridional streamlines, and (b)  $w$ -component at the axis of rotation.

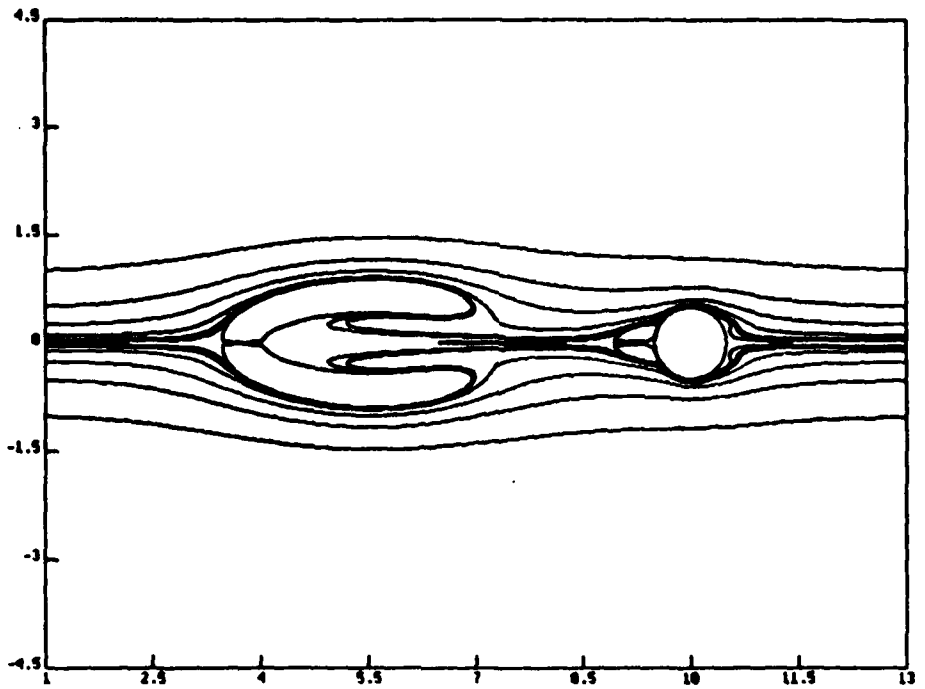


Fig. 20. Meridional streamlines for  $Re = 500$ ,  $S = 0.80$  with a sphere.

## REFERENCES

1. Skow, A.M. and A. Titiriga, "A Survey of Analytical and Experimental Techniques to Predict Aircraft Dynamic Characteristics at High Angles of Attack," AGARD-CP 235, No. 19 (1978).
2. Gupta, A.K., D.G. Lilley, and N. Syred, "Swirl Flows," Abacus Press, Tunbridge Wells, Kent (1984).
3. Falor, J.H. and S. Leibovich, "Disrupted States of Vortex Flows and Vortex Breakdown," Phys. Fluids, 20, 1385 (1977).
4. Benjamin, T.B., "Theory of the Vortex Breakdown Phenomenon," J. Fluid Mech., 14, 593 (1962).
5. Lugt, H.J., "Einfluss der Drallströmung auf die Durchflusszahlen genormter Drosselmessgeräte," PhD Thesis, Stuttgart (1959). Abbreviated version translated by the British Hydromechanics Research Association, Rep. T 716 (Feb 1962).
6. Wedemeyer, E., "Vortex Breakdown," AGARD-VKI Lecture Series 121 Paper 9-1 (1982).
7. Leibovich, S., "Vortex Stability and Breakdown: Survey and Extension," AIAA J., 22, 1192 (1984).
8. Escudier, M.P., J. Bornstein, and T. Maxworthy, "The Dynamics of Confined Vortices," Proc. Roy. Soc., A 382, 335 (1982).
9. Leibovich, S., "Wave Propagation, Instability, and Breakdown of Vortices," Vortex Motion, Eds: H.G. Hornung and E.-A. Müller, Vieweg, Braunschweig, 50 (1982).
10. Escudier, M.P. and J.J. Keller, "Vortex Breakdown: A Two-Stage Transition," AGARD-CP 342 (1983).
11. Hall, M.G., "Vortex Breakdown," Ann. Rev. Fluid Mech., 4, 195 (1972).
12. Kopecky, R.M. and K.E. Torrance, "Initiation and Structure of Axisymmetric Eddies in a Rotating Stream," Comp. Fluids, 1, 289 (1973).
13. Grabowski, W.J. and S.A. Berger, "Solutions of the Navier-Stokes Equations for Vortex Breakdown," J. Fluid Mech., 75, 525 (1976).
14. Menne, S., "Vortex Breakdown in an Axisymmetric Flow," AIAA Paper No. 88-0506 (1988).
15. Escudier, M.P., "Observations of the Flow Produced in a Cylindrical Container by a Rotating End Wall," Exp. Fluids, 2, 189 (1984).
16. Lugt, H.J. and H.J. Haussling, "Axisymmetric Vortex Breakdown in Rotating Fluid Within a Container," J. Appl. Mech., ASME, 49, 921 (1982).

17. Lugt, H.J. and M. Abboud, "Axisymmetric Vortex Breakdown With and Without Temperature Effects in a Container With a Rotating Lid," *J. Fluid Mech.*, 179, 179 (1987).
18. Escudier, M.P. and J.J. Keller, "Recirculation in Swirling Flow: A Manifestation of Vortex Breakdown," *AIAA J.*, 23, 111 (1985).
19. Chao, Y.C., "Recirculation Structure of the Coannular Swirling Jets in a Combustor," *AIAA J.*, 26, 623 (1988).
20. Owen, J.M. and J.R. Pincombe, "Vortex Breakdown in a Rotating Cylindrical Cavity," *J. Fluid Mech.*, 90, 109 (1979).
21. Phillips, W.R.C., "On Vortex Boundary Layers," *Proc. Roy. Soc., A* 400, 253 (1985).
22. Maxworthy, T., "The Flow Created by a Sphere Moving Along the Axis of a Rotating, Slightly-Viscous Fluid," *J. Fluid Mech.*, 40, 453 (1970).
23. Lugt, H.J., "Vortex Flow in Nature and Technology," Wiley-Interscience, New York (1983).
24. Spall, R.E., T.B. Gatski, and C.E. Grosch, "A Criterion for Vortex Breakdown," *Phys. Fluids*, 30, 3434 (1987).
25. Squire, H.B., "Analysis of the 'Vortex Breakdown' Phenomenon," Part 1, *Aero. Dept., Imperial Coll., London, Rep.* 102 (1960).
26. Chorin, A.J., "A Numerical Method for Solving Incompressible Viscous Flow Problems," *J. Comp. Phys.*, 2, 12 (1967).
27. Chakravarthy, S.R. and S. Osher, "A New Class of High Accuracy TVD Schemes for Hyperbolic Conservation Laws," *AIAA Paper No. 85-0363* (1985).
28. Chakravarthy, S.R. and D.K. Ota, "Numerical Issues in Computing Inviscid Supersonic Flow Over Conical Delta Wings," *AIAA Paper No. 86-0440* (1986).
29. Gorski, J.J., "TVD Solutions of the Incompressible Navier-Stokes Equations With an Implicit Multigrid Scheme," *AIAA Paper No. 88-3699* (1988).
30. Purtell, L.P. and S. Fish, "Experiments on Induced Breakdown of a Tip Vortex," Presented at the Fortieth Annual Meeting of the Division of Fluid Dynamics, American Physical Society, Eugene, Oregon (22-24 Nov 1987).

## INITIAL DISTRIBUTION

### Copies

1 DARPA  
1 H.S. Wisniewski

1 Library of Congress  
1 Science and Tech Division

4 ONR  
1 R. Whitehead  
1 J. Fein  
1 E.P. Rood  
1 M. Reischmann

2 NASA Langley Res Center  
1 D. Bushnell  
1 T.B. Gatski

3 NAVSEA  
1 SEA 05, RADM Ricketts  
1 W. Sandberg  
1 Lib

1 NASA Ames Res Center  
1 B.G. McLachlan

2 USNA  
1 R.A. Granger  
1 Tech Lib

1 NASA Lewis Res Center/Lib

1 Air Force Flight Dynamics Lab/Lib  
1 U.S. Army Ballistic Res Lab  
1 C.W. Kitchens

1 NRL  
1 O.M. Griffin

1 NIST/Lib

1 NAVPGSCOL  
1 Lib

1 NSWC/Dahlgren/Lib

1 NSWC/Whiteoak/Lib

1 Naval Ship Eng Cent Tech Lib

12 DTIC

CENTER DISTRIBUTION

Copies Code Name

1	00	C. Graham
1	01	R. Metrey
1	01A	D.D. Moran
1	01B	D.J. Clark
1	011	E. O'Neill
5	0113	W. Lukens
1	0117	B. Nakonechny
1	15	W.B. Morgan
1	152	W.-C. Lin
1	154	J.H. McCarthy
1	1542	T.T. Huang
1	1543	L.P. Purtell
1	156	D.S. Cieslowski
1	16	H.R. Chaplin
1	18	C.M. Schoman
20	1802	H.J. Lugt
1	184	J.W. Schot
1	1843	H.J. Haussling
20	1843	J.J. Gorski
10	5211.1	Reports Control
1	522.1	TIC (C)
1	522.2	TIC (A)